J Biol Inorg Chem (2010) 15:1305–1318
DOI 10.1007/s00775-010-0690-6

ORIGINAL PAPER

Boronated phosphonium salts containing arylboronic acid, *closo*-carborane, or *nido*-carborane: synthesis, X-ray diffraction, in vitro cytotoxicity, and cellular uptake

Daniel E. Morrison · Fatiah Issa · Mohan Bhadbhade · Ludwig Groebler · Paul K. Witting · Michael Kassiou · Peter J. Rutledge · Louis M. Rendina

Received: 23 February 2010 / Accepted: 8 July 2010 / Published online: 6 August 2010

Abstract The preparation of boronated triaryl and tetraaryl phosphonium salts of the type $[PPh_3CH_2R]Br$ [*R* is 4-boronophenyl (**1**), 4-(4,4,5,5-tetramethyl-1,3,2-dioxaborolan-yl)phenyl (**2**), 3-boronophenyl (**3**), 3-(4,4,5,5-tetramethyl-1,3,2-dioxaborolan-yl)phenyl (**4**), 2-boronophenyl (**5**), 2-(4,4,5,5-tetramethyl-1,3,2-dioxaborolan-yl)phenyl (**6**), and *closo*-1,2-carboran-1-yl (**7**)] is described. These compounds were prepared by the reaction of triphenylphosphine with benzylic bromides or 1-bromomethyl-*closo*-1,2-carborane in acetonitrile solution at 85 °C. The zwitterionic *nido*-7,8-carborane derivative $PPh_3CH_2C_2B_9H_{11}$ (**8**) was prepared by treatment of **7** with cesium fluoride in refluxing ethanol. All compounds were fully characterized by multinuclear (^1H, ^{11}B, ^{13}C, and ^{31}P) 1D- and 2D-NMR spectroscopy, electrospray ionization mass spectrometry, and elemental analysis, and single-crystal X-ray structures were determined for compounds **1**, **3**, **7**, and **8**. The cytotoxicities and boron uptake of selected derivatives were investigated in vitro using human glioblastoma (T98G) and canine kidney tubule (MDCK II) cells. The zwitterionic species **8** was found to be the least cytotoxic agent while also delivering the greatest amount of boron to the T98G cells, peaking at 9.15 ± 2.65 μg B/mg protein.

Keywords Boron neutron capture therapy · Carborane · Boronic acid · Phosphonium salt · Mitochondria

Introduction

Boron neutron capture therapy (BNCT) is an experimental cancer treatment which is primarily used to treat tumors of the CNS, most commonly the intractable and aggressive brain malignancy known as glioblastoma multiforme [1–3]. The therapy is highly reliant upon ^{10}B agents which can

D. E. Morrison and F. Issa contributed equally to this work.

Electronic supplementary material The online version of this article (doi:10.1007/s00775-010-0690-6) contains supplementary material, which is available to authorized users.

D. E. Morrison · F. Issa · M. Kassiou · P. J. Rutledge · L. M. Rendina (✉)
School of Chemistry,
The University of Sydney,
Sydney, NSW 2006, Australia
e-mail: lou.rendina@sydney.edu.au

M. Bhadbhade
Solid State and Elemental Analysis Unit,
The University of New South Wales,
Kensington, NSW 2052, Australia

L. Groebler · P. K. Witting
Discipline of Pathology,
School of Medical Sciences,
The University of Sydney, Sydney,
NSW 2006, Australia

M. Kassiou
Discipline of Medical Radiation Sciences,
Faculty of Health Sciences,
The University of Sydney,
Cumberland Campus,
Lidcombe, NSW 2141, Australia

M. Kassiou
Brain and Mind Research Institute,
The University of Sydney,
Camperdown, NSW 2050, Australia

localize within tumor cells prior to irradiation with thermal neutrons, resulting in neutron capture by a ^{10}B nucleus and the liberation of an α particle and a ^{7}Li ion, a process which is accompanied by a considerable amount of kinetic energy. Selective uptake of boronated compounds into tumor cells would significantly enhance the probability of a neutron capture reaction with ^{10}B, ultimately leading to an enhanced tumor cell kill. The search for new agents that can selectively target tumors and deliver sufficient quantities of boron to critical tumor cell components such as DNA and mitochondria is ongoing. Delocalized lipophilic cations (DLCs) are known to accumulate selectively in the mitochondria of tumor cells owing to a significant difference in the mitochondrial membrane potential between tumor cells and normal, healthy cells [4–7]. Numerous DLCs have been assessed for their anticancer properties [4, 8–14], with selected examples entering human clinical trials [4]. However, the study of DLCs as potential boron carriers for BNCT is a more recent development. The first reported instance of a boron-containing DLC was the *closo*-1,12-carborane-containing analogue of dequalinium chloride, which was found to accumulate selectively in human epidermoid carcinoma of the oral cavity and rat glioma in vitro, exhibiting uptake and retention properties similar to those of rhodamine 123, MKT-077, and tetraphenylphosphonium (TPP) chloride (Fig. 1) [15]. More recently, it has been shown that an anionic *nido*-7,8-carborane can be used as a counterion in selected DLC salts that exhibit favorable tumor selectivity, a strategy that has allowed selective boron uptake in human prostate epithelial carcinoma in vitro [16].

Of the DLCs studied to date, phosphonium ions such as TPP and triphenylmethylphosphonium (TPMP) have demonstrated particularly high selectivity toward glioma in vivo [17–19]. By comparison, 4-boronophenylalanine and sodium mercaptoundecahydrododecaborate(−1) ($Na_2[B_{12}H_{11}SH]$; BSH) (Fig. 2), two boronated agents used in clinical trials for BNCT, have shown at best a tumor to healthy tissue selectivity of 6.4:1 when used in tandem [20]. Thus, boronated phosphonium salts, in particular analogues of TPP and TPMP, may offer distinct advantages as BNCT agents and may allow significantly enhanced boron uptake by tumor cells, a key factor in enhancing the efficacy of this cancer therapy.

Previous work by Ioppolo et al. [21] led to the first arylphosphonium salts containing a *closo*-carborane or *nido*-carborane cage α to the phosphonium center. These compounds demonstrated favorable in vitro cytotoxicity during preliminary anticancer screening against the SF268 human glioblastoma line. Herein, we report the synthesis and preliminary biological evaluation of two new classes of boronated phosphonium derivatives (Fig. 3): salts in which the boron moiety is an arylboronic acid or ester derivative,

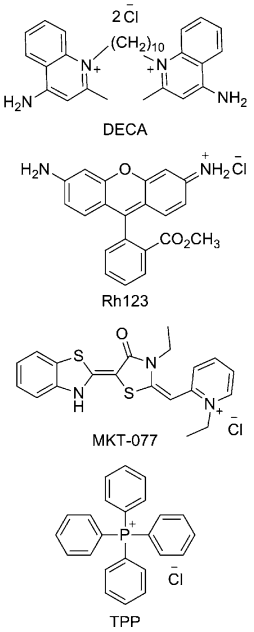

Fig. 1 Structures of dequalinium chloride (*DECA*), rhodamine 123 (*Rh123*), MKT-077, and tetraphenylphosphonium chloride (*TPP*)

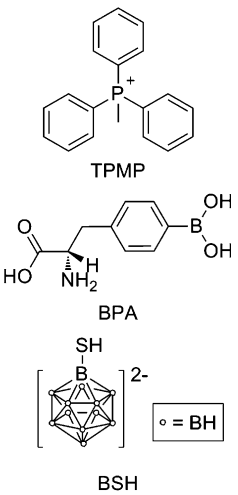

Fig. 2 Structures of the triphenylmethylphosphonium (*TPMP*) cation, 4-boronophenylalanine (*BPA*), and sodium mercaptoundecahydrododecaborate(−1) (*BSH*)

and compounds incorporating a methylenecarborane species in which the phosphorus is not directly linked to the boron cluster. This structural change would necessarily influence delocalization of the cationic charge associated with the phosphonium center and may lead to significant changes in reactivity (e.g., deboronation of the *closo*-carborane cage) [21], and changes in uptake by tumor cell mitochondria. Modification of the boronic acid derivatives by condensation with a diol such as pinacol, or complex formation with sugars such as D-fructose, allows the boronic acid to be masked with either a more lipophilic or a more hydrophilic group, respectively, and thus provides further scope for tailoring drug activity. We also report the in vitro biological activity of selected derivatives toward the T98G human glioblastoma multiforme cell line and

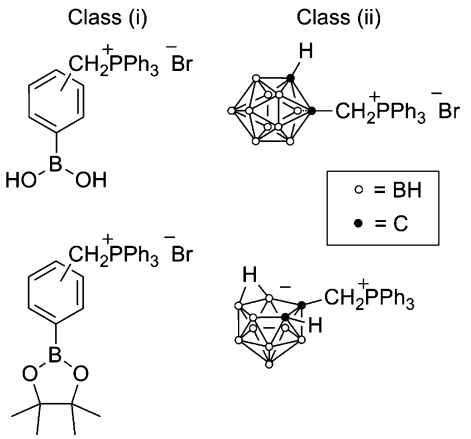

Fig. 3 The two classes of compounds investigated in this study: arylboronic acid derivatives (*i*) and methylcarborane derivatives (*ii*)

assess the potential nephrotoxicity of these cations using cultured kidney tubule epithelial cells (Madin–Darby canine kidney type II; MDCK II). The selectivity of phosphonium salts, determined as a ratio of IC_{50} values for MDCK II and T98G cell lines, is also reported [22]. Finally, the results from a boron uptake study of selected derivatives by T98G cells are provided.

Results and discussion

Syntheses

The synthesis of the benzylphosphonium salts (4-boronobenzyl)triphenylphosphonium bromide (**1**), triphenyl(4-(4,4,5,5-tetramethyl-1,3,2-dioxaborolan-2-yl)benzyl)phosphonium bromide (**2**), (3-boronobenzyl)triphenylphosphonium bromide (**3**), triphenyl(3-(4,4,5,5-tetramethyl-1,3,2-dioxaborolan-2-yl)benzyl)phosphonium bromide (**4**), (2-boronobenzyl)triphenylphosphonium bromide (**5**), and triphenyl (2-(4,4,5,5-tetramethyl-1,3,2-dioxaborolan-2-yl)benzyl) phosphonium bromide (**6**) was achieved using a facile nucleophilic substitution reaction of boronated alkyl bromide precursors with triphenylphosphine [23, 24]. The desired phosphonium salts containing either the free acid (**1**, **3**, and **5**) or pinacol ester (**2**, **4**, and **6**) were readily prepared in high yield (83–97%) and purity (Schemes 1, 2). A similar route proved ineffective for the preparation of the carborane-containing compound (*closo*-1,2-carboran-1-ylmethyl)triphenylphosphonium bromide (**7**). This is presumably due to the strongly electron withdrawing character of the *closo*-carborane cage in the 1-bromomethyl-*closo*-1,2-carborane precursor, which would decrease the rate of the substitution reaction. As a result, the reaction of 1-bromomethyl-*closo*-1,2-carborane (**15**) and triphenylphosphine did not afford the

Scheme 1 Reagent: *i* PPh_3

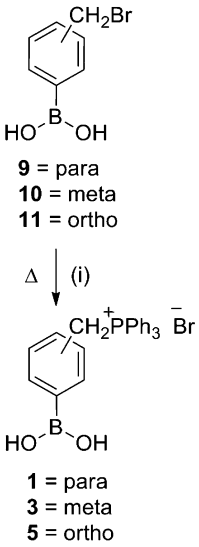

Scheme 2 Reagents: *i* pinacol, *ii* PPh_3

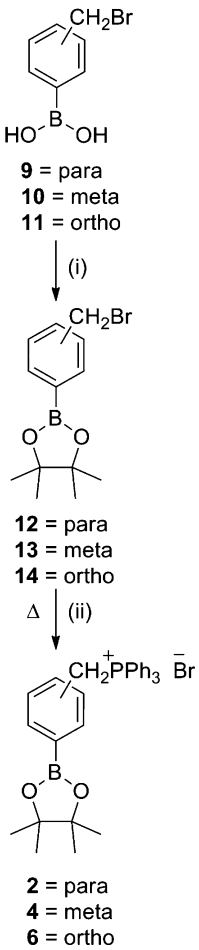

desired product, and undesired side reactions were found to dominate. This diminished reactivity is typical of halomethyl-*closo*-carboranes, and indeed a slow rate of halide substitution has been observed previously in the preparation of methyl-*closo*-carborane-derived Grignard reagents

Scheme 3 Reagents: *i* PPh_3, *ii* CsF, EtOH

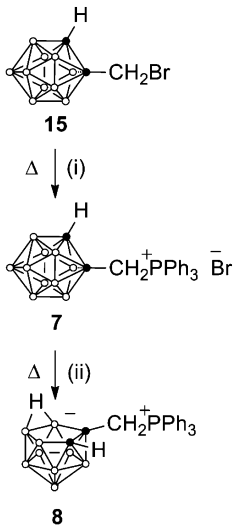

[25, 26]. Instead, the *closo*-1,2-carborane-containing phosphonium salt **7** was prepared by performing the reaction at high temperature in the absence of solvent, an alternative method to that previously reported by Kalinin et al. [27]. The *closo*-1,2-carborane species was selectively deboronated using cesium fluoride to afford the zwitterionic (7,8-dicarba-*nido*-undecaborane-7-ylmethyl)triphenylphosphonium (**8**) in high yield and purity (Scheme 3) [28].

All compounds were characterized by a combination of multinuclear (^{1}H, ^{11}B, ^{13}C, and ^{31}P) 1D- and 2D-NMR spectroscopy, electrospray ionization (ESI) mass spectrometry (MS), and elemental analysis, and in the case of compounds **1**, **3**, **7**, and **8**, X-ray structures were also determined. The ^{1}H NMR resonances due to the methylene protons in both reagent and product gave a clear indication of product formation owing to the appearance of ^{31}P coupling. These proton signals appear in the range δ 4.89–5.63 for the free boronic acids **1**, **3**, and **5** and in the range δ 5.38–5.63 for the corresponding pinacol esters **2**, **4**, and **6**, and display characteristic ^{31}P coupling ($^2J_{H-P}$ = 14.2–15.6 Hz). In addition, a singlet was observed in the ^{31}P{^{1}H} NMR spectrum in the range δ 24.2–28.4 for the boronic acids **1**, **3**, and **5** and in the range δ 24.2–24.9 for the pinacol esters **2**, **4**, and **6**, characteristic of a quaternary aryl phosphonium species [29]. ESI-MS provided further evidence for the formation of the desired salts: derivatives containing boronic acid were observed as either singly or doubly condensed esters of solvent MeOH, whereas the pinacol ester derivatives were detected as clusters of parent species with the loss of one bromide ion, i.e., $[M–Br]^+$ and $[2M–Br]^+$.

The ^{1}H, ^{1}H{^{31}P}, and ^{31}P{^{1}H} NMR spectra of the carborane-containing species **7** and **8** showed features similar to those reported above. For **7**, the methylene proton signal appeared at δ 5.60 ($^2J_{H-P}$ = 14.3 Hz), significantly downfield from the signal for the corresponding protons in the 1-bromomethyl-*closo*-1,2-carborane (**15**) precursor at δ 3.96. In the ^{1}H NMR spectrum of **8**, two distinct doublet-of-doublet signals at δ 4.18 and 3.62 can be attributed to the diastereotopic methylene protons. These protons were coupled to each other with a coupling constant $^2J_{H-H}$ = 16.5 Hz (consistent with geminal coupling), and to the phosphorus. Each signal was resolved into a simple doublet in the ^{1}H{^{31}P} NMR spectrum. Both **7** and **8** gave typical ^{31}P signals for arylphosphonium compounds at δ 22.8 and 23.4, respectively [29]. A clear distinction between the *closo*-carborane and *nido*-carborane cages was apparent in the ^{11}B{^{1}H} NMR spectra. For the monosubstituted *closo*-1,2-carborane **7**, three signals were observed in the ^{11}B{^{1}H} NMR spectrum between δ −2.7 and −12.0, typical for asymmetrically substituted *closo*-carborane cages [30]. For the monosubstituted *nido*-7,8-carborane **8**, the resonances appeared further upfield in the range δ −8.5 to −35.3, characteristic of *nido*-carborane cages [31]. The *nido*-carborane cage was further confirmed by the presence of an upfield signal at δ −3.60 in the ^{1}H{^{11}B} NMR spectrum, assigned to the *endo*-bridging hydrogen atom [21, 32].

X-ray diffraction studies

In addition to NMR and ESI-MS characterization, single-crystal X-ray crystallography of the boronic acid containing phosphonium salts **1** (Fig. 4) and **3** (Fig. 5) and carborane-containing species **7** (Fig. 6) and **8** (Fig. 7) confirmed their molecular structures. The boronate esters **2** and **4** underwent facile hydrolysis during crystallization to afford boronic acids **1** and **3**, respectively. Whereas the hydrolysis of **4** led to crystals which were identical to those obtained directly from **3**, the hydrolysis of **2** resulted in a polymorphic form of **1** (denoted as **1′**). The structure of **1′** is presented in the electronic supplementary material.

The X-ray crystal structures of **1** and **3** closely resemble that of the related $[PPh_3CH_2Ph]^+$ species with regard to bond parameters about the phosphorus atom and torsion angles about the P–CH_2 bond [33]. Both **1** and **3** adopt a similar distorted staggered conformation about this bond, with torsion angles of −56.7° and −52.9° between the benzyl and phenyl groups, respectively. The phosphorus atom in both structures deviates marginally from an ideal tetrahedral geometry, with bond angles from 107.7(1)° to 111.4(1)° and from 106.0(3)° to 112.6(3)° for **1** and **3**, respectively. The P–C_{aryl} bond lengths range from 1.794(2) to 1.803(2) Å (**1**) and from 1.779(6) to 1.809(6) Å (**3**), comparable to those found in the $[PPh_3CH_2Ph]Br$ salt [from 1.789(4) to 1.797(4) Å] [33]. The P–CH_2 bond

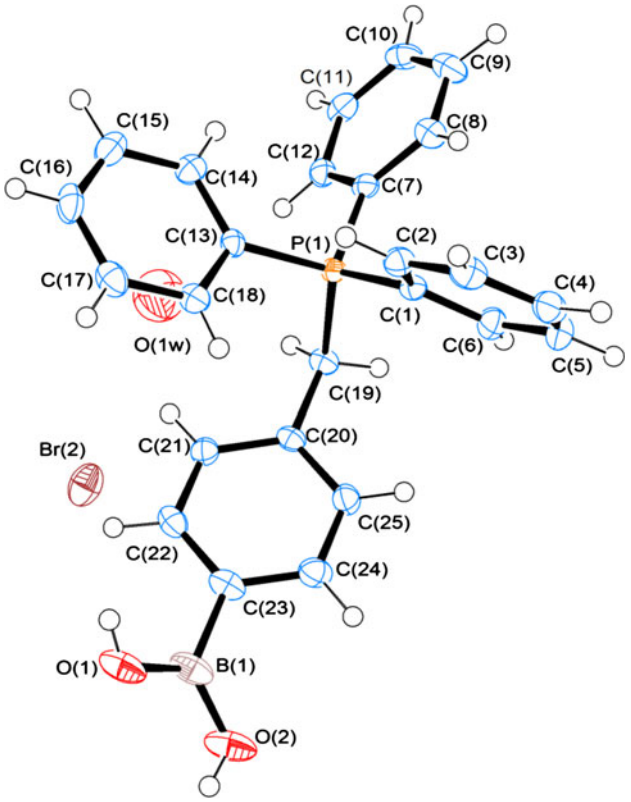

Fig. 4 An ORTEP depiction and atomic numbering scheme of (4-boronobenzyl)triphenylphosphonium bromide (**1**) with 50% displacement ellipsoids. Selected bond lengths (Å): C(1)–P(1) = 1.794(2), C(7)–P(1) = 1.803(2), C(13)–P(1) = 1.799(2), C(19)–C(20) = 1.508(3), C(19)–P(1) = 1.821(2). Selected bond angles (deg): C(1)–P(1)–C(7) = 109.6(1), C(1)–P(1)–C(13) = 109.2(1), C(1)–P(1)–C(19) = 110.1(1), C(7)–P(1)–C(13) = 108.8(1), C(7)–P(1)–C(19) = 107.7(1), C(13)–P(1)–C(19) = 111.4(1), C(20)–C(19)–P(1) = 113.4(2). Selected torsion angles (deg): C(20)–C(19)–P(1)–C(1) = 64.7, C(20)–C(19)–P(1)–C(7) = −175.9, C(20)–C(19)–P(1)–C(13) = −56.7

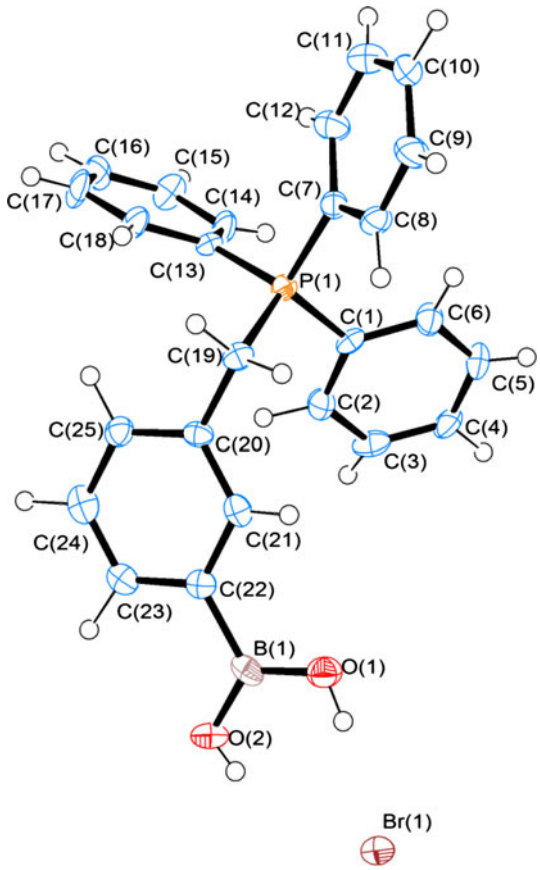

Fig. 5 An ORTEP depiction and atomic numbering scheme of (3-boronobenzyl)triphenylphosphonium bromide (**3**) with 50% displacement ellipsoids. Selected bond lengths (Å): C(1)–P(1) = 1.779(6), C(7)–P(1) = 1.809(6), C(13)–P(1) = 1.791(6), C(19)–P(1) = 1.822(6), C(19)–C(20) = 1.503(8). Selected bond angles (deg): C(1)–P(1)–C(7) = 112.6(3), C(1)–P(1)–C(13) = 107.7(3), C(1)–P(1)–C(19) = 111.1(3), C(7)–P(1)–C(13) = 108.7(3), C(7)–P(1)–C(19) = 106.0(3), C(13)–P(1)–C(19) = 110.7(3), C(20)–C(19)–P(1) = 117.5(4). Selected torsion angles (deg): C(20)–C(19)–P(1)–C(1) = –52.9, C(20)–C(19)–P(1)–C(7) = –175.5, C(20)–C(19)–P(1)–C(13) = 66.8

lengths are 1.821(2) and 1.822(6) Å (**1** and **3**, respectively), compared with 1.802(4) Å for $[PPh_3CH_2Ph]Br$ [33].

The orientations of the phenyl rings in the structures vary greatly between **1** and **3** and relative to the related species $[PPh_3CH_2Ph]Br$ [33]. The relative orientation of the rings can be compared in two ways. The dihedral angle between the plane of the benzyl ring and the plane formed by carbon atoms C(1), C(7), and C(13) gives an indication of the orientation of the benzyl ring relative to the rest of the molecule. These dihedral angles are 24.3(0)° and 36.4(6)° for **1** and **3**, respectively. The value for **3** shows considerable deviation from the corresponding dihedral angle observed in $[PPh_3CH_2Ph]X$ (29.3°, 24.2°, and 24.8° for the X = chloride, bromide, and iodide salts, respectively) [33]. Alternatively, considering the dihedral angle between the planes of the benzyl ring and the adjacent phenyl rings gives an indication of the relative rotation of aryl rings relative to each other. For **1**, these angles are 71.1(1)°, 45.6(3)°, and 24.8(9)° and for **3** they are 47.0(8)°, 43.0(1)°, and 87.1(7)°.

In the carborane species **7** and **8**, the P–CH_2 bond lengths are 1.823(2) and 1.813(4) Å, respectively, comparable to the P–CH_2 bond length in $[PPh_3CH_2Ph]Br$ [1.802(4) Å] [33], but both are considerably elongated relative to the P–CHPh bond of the ylide PPh_3CHPh [1.696(3) Å] [34]. The similar P–CH_2 bond lengths observed in **7** and **8** provides strong support for a zwitterionic structure for the latter, in which separate but delocalized positive and negative charges are centered at the triphenylphosphonium moiety and the *nido*-7,8-carborane cage, respectively (as has been previously observed for the related species PPh_2Me-7,8-$C_2B_9H_{11}$) [21]. Indeed, the marginal shortening of the P–CH_2 bond in **8** compared with **7** indicates that, in the former, this bond possesses very little double-bond character. Compounds **7**

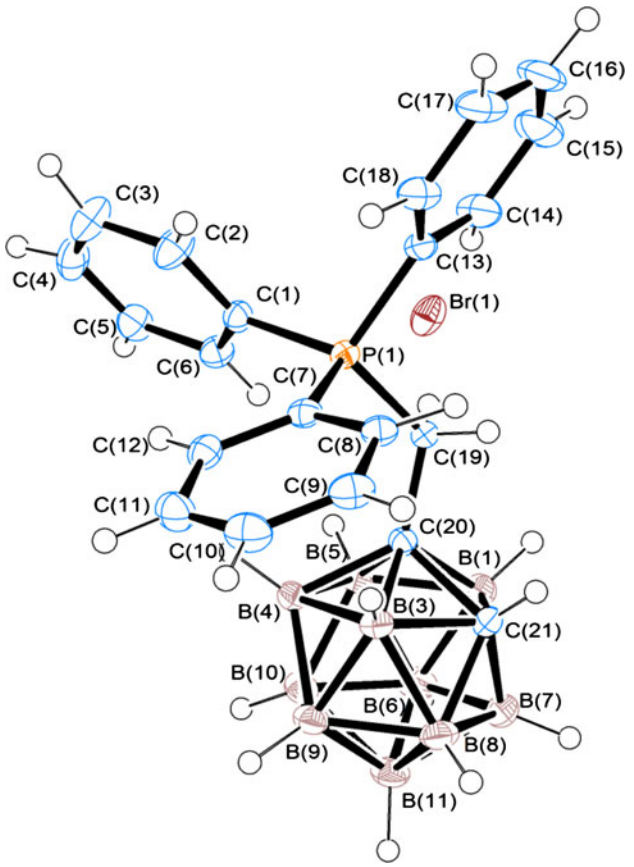

Fig. 6 An ORTEP depiction and atomic numbering scheme of (*closo*-1,2-carboran-1-ylmethyl)triphenylphosphonium bromide (**7**) with 50% displacement ellipsoids. Selected bond lengths (Å): P(1)–C(1) = 1.787(2), P(1)–C(7) = 1.791(2), P(1)–C(13) = 1.797(2), P(1)–C(19) = 1.823(2), C(19)–C(20) = 1.523(3). Selected bond angles (deg): C(1)–P(1)–C(7) = 108.3(1), C(1)–P(1)–C(13) = 108.7(1), C(1)–P(1)–C(19) = 113.7(1), C(7)–P(1)–C(13) = 109.9(1), C(7)–P(1)–C(19) = 111.9(1), C(13)–P(1)–C(19) = 104.2(1), P(1)–C(19)–C(20) = 122.7(2). Selected torsion angles (deg): C(1)–P(1)–C(19)–C(20) = –78.0, C(7)–P(1)–C(19)–C(20) = 45.1, C(13)–P(1)–C(19)–C(20) = 163.8

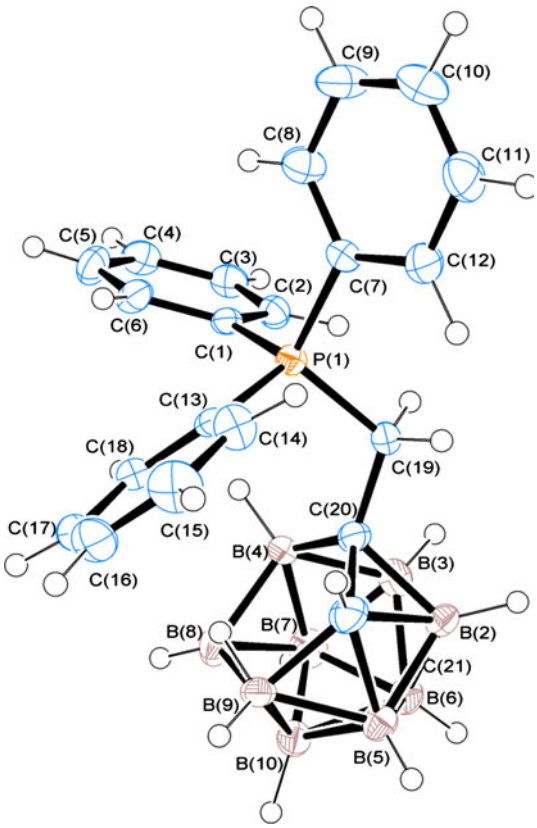

Fig. 7 An ORTEP depiction and atomic numbering scheme of (7, 8-dicarba-*nido*-undecaborane-7-ylmethyl)triphenylphosphonium (**8**) with 50% displacement ellipsoids. Selected bond lengths (Å): C(1)–P(1) = 1.800(3), C(7)–P(1) = 1.806(3), C(13)–P(1) = 1.792(4), C(19)–P(1) = 1.813(4), C(19)–C(20) = 1.531(5). Selected bond angles (deg): C(1)–P(1)–C(7) = 108.6(2), C(1)–P(1)–C(13) = 110.1(2), C(1)–P(1)–C(19) = 111.4(2), C(7)–P(1)–C(13) = 109.4(2), C(7)–P(1)–C(19) = 108.3(2), C(13)–P(1)–C(19) = 108.9(2), C(20)–C(19)–P(1) = 114.5(3). Selected torsion angles (deg): C(20)–C(19)–P(1)–C(1) = –77.3, C(20)–C(19)–P(1)–C(7) = 163.3, C(20)–C(19)–P(1)–C(13) = 44.4

and **8** share a similar conformation about the P–CH_2 bond axis, in which the carborane cage is in an almost staggered conformation relative to the phenyl rings at phosphorus. The torsion angles are 45.1° and 44.4° between the carborane and adjacent phenyl rings, which are orientated such that the plane of each ring is almost perpendicular to the carborane cage. The bond angles and lengths of both compounds are comparable to those of typical $[PPh_3CH_2R]^+$ salts such as $[PPh_3CH_2Ph]Br$ [33, 35]. The central phosphorus atom is close to tetrahedral in both compounds: in **7** the bond angles range from 104.2(1)° [C(13)–P(1)–C(19)] to 113.7(1)° [C(1)–P(1)–C(19)], whereas in **8** they range from 108.3(2)° [C(7)–P(1)–C(19)] to 111.4(2)° [C(1)–P(1)–C(19)]. The significant distortion exhibited by both compounds relative to $[PPh_3CH_2Ph]^+$ is a direct result of the carborane cage [33]. The steric bulk of the *closo*-carborane in **7** causes an increase in the bond angles between the cage and adjacent phenyl rings [C(1)–P(1)–C(19), C(7)–P(1)–C(19), P(1)–C(19)–C(20)] and a decrease of the complementary C(13)–P(1)–C(19) bond angle. This contrasts with the structure of **8**, where the reverse is observed: there is a relative decrease in the bond angles between the *nido*-carborane and adjacent phenyl rings [C(7)–P(1)–C(19), C(13)–P(1)–C(19), P(1)–C(19)–C(20)], whereas the complementary C(1)–P(1)–C(19) bond angle is increased. The overall distortion resulting from these effects is smaller in **8** than in **7**. This reversal can be attributed to the reduction in overall steric bulk of the cage owing to the presence of an open (*nido*) rather than a closed (*closo*) face, plus electrostatic attraction between the delocalized negative charge of the cage and the positively charged phosphonium center in **8**. This contrast between **7** and **8** is also evident in the distance between the substituted carbon atom of the cage and the *ipso* carbon of the

adjacent phenyl ring. In **7** this distance [C(20)···C(7)] is 3.51(6) Å, whereas the corresponding distance in **8** [C(20)···C(13)] is shortened to 3.25(9) Å. The relative bulk of the two carboranes is also apparent in the intramolecular distances between the carborane hydrogen atoms and ring centroids of adjacent aromatic rings. In **7**, the intramolecular B(3)H···ring centroid [C(7)-containing ring] distance is 2.60(3) Å compared with 2.90(9) Å in **8**. This parameter further demonstrates the reduced size of the *nido*-carborane cage compared with that of the *closo*-carborane. Finally, the carborane open-face centroid···ring centroid [C(13)-containing ring] distance in **8** is 3.88(4) Å, with an inclination of 19.5(3)° between these planes.

In vitro cytotoxicity and cell uptake studies with T98G glioblastoma cells

The mean in vitro cytotoxicities of **1** and **2** were determined using the T98G human glioblastoma cell line and were found to be similar, with IC_{50} values of 10.1 ± 1.1 μM ($n = 16$ from four experiments) and 15.8 ± 0.4 μM ($n = 12$ from three experiments), respectively (Table 1, entries 1, 2). In vitro cytotoxicity screening of **7** and **8** against the same cell line demonstrates that the *closo*-carborane derivative **7** is approximately 3 times more toxic than the corresponding *nido* derivative **8**, as determined by the respective mean IC_{50} values of 21.1 ± 5.4 μM ($n = 12$ replicates from three independent experiments) and 60.6 ± 19.0 μM ($n = 12$ from three independent experiments) (Table 1, entries 3, 4). By comparison, the viability profile of T98G cells treated with the clinically used agent BSH showed that this compound was nontoxic to cells even at doses as high as 800 μM, although its tumor selectivity is only marginal [3]. One-way analysis of variance (nonparametric) using the Newman–Keuls multiple-comparison test showed the difference in IC_{50} values of the *nido*-carborane derivative **8** treatment arm is statistically significant at a 95% confidence level ($p < 0.05$) to the treatment arms of **1**, **2**, and **7**. In contrast, compounds **1**, **2**, **7**, and **8** displayed much lower cytotoxic effects toward cultured MDCK II cells (Table 2), a result which is consistent with the reported difference in the mitochondrial membrane potentials of normal and cancerous cells [4–7]. Evidence for the interaction of cationic arylphosphonium salts with DNA and its correlation with cytotoxicity has recently been reported [36]. Indeed, secondary cytotoxic effects associated with the interaction of boronated phosphonium compounds with chromosomal DNA in the absence of neutrons may potentially prove useful when coupled with BNCT in the clinic.

The in vitro selectivity of delocalized cations for cultured cancer cells relative to kidney epithelial cells was first reported by Rideout et al. [22] as a ratio of IC_{50} values. Using this approach, the in vitro selectivity of phosphonium salts **1** and **2** were calculated to be 8.7 and 8.6, respectively, whereas the selectivity of **7** was determined to be more than 5.9 (Table 3). Owing to the low aqueous solubilities of **7** and **8**, doses above 125 μM were not investigated and thus accurate IC_{50} values from a required sigmoidal dose–response could not be determined for the MDCK II cell line (Table 2). One should exercise some degree of caution in interpreting the selectivity value (more

Table 1 In vitro cytotoxicity of (4-boronobenzyl)triphenylphosphonium bromide (**1**), triphenyl(4-(4,4,5,5-tetramethyl-1,3,2-dioxaborolan-2-yl)benzyl)phosphonium bromide (**2**), (closo-1,2-carboran-1-ylmethyl)triphenylphosphonium bromide (**7**), (7,8-dicarba-nido-undecaborane-7-ylmethyl)triphenylphosphonium (**8**), and sodium mercaptoundecahydrododecaborate(−1) (*BSH*) toward the human glioblastoma (T98G) cell line

Entry	Compound	IC_{50} (μM) (±SE, *n*)
1	**1**	10.1 (1.1, $n = 4$)
2	**2**	15.8 (0.4, $n = 3$)
3	**7**	21.1 (5.4, $n = 3$)
4	**8**	60.6 (19, $n = 3$)
5	BSH	>800 ($n = 3$)

SE standard error

Table 2 In vitro cytotoxicity of **1**, **2**, **7**, **8**, and BSH toward the Madin–Darby canine kidney type II (MDCK II) cell line

Entry	Compound	IC_{50} (μM) (±SE, *n*)
1	**1**	88.1 (19.5, $n = 3$)
2	**2**	136.6 (41.5, $n = 3$)
3	**7**[a]	>125 ($n = 3$)
4	**8**[a]	>125 ($n = 3$)
5	BSH[a]	>800 ($n = 3$)

[a] Sigmoidal dose–response curves could not be determined owing to the low water solubility of compounds **7** and **8** at high concentrations and the nontoxic behavior of BSH

Table 3 In vitro selectivity of **1**, **2**, **7**, **8**, and BSH

Entry	Compound	Selectivity (IC_{50} MDCK II/IC_{50} T98G)
1	**1**	8.7 (2.2)
2	**2**	8.6 (2.6)
3	**7**	>5.9 (NR[a])
4	**8**	>2.1 (NR[a])
5	BSH	ND[b]

[a] The error value is not reported (*NR*) because an accurate IC_{50} value could not be determined owing to the low aqueous solubility of the compound at higher concentrations

[b] Could not be determined (*ND*) as MDCK II and T98G cells were unaffected when treated with a 800 μM concentration of the compound

than 2.1) for that of the zwitterionic salt **8** relative to those of the other phosphonium salts because the compound lacks an overall charge and thus it is unlikely to exhibit the same mechanism of action as that of the cationic species.

Preliminary cell uptake studies were conducted to correlate cytotoxicity with the extent of boron uptake into the cultured T98G cells. Treatment of T98G cells with **7** or **8** (10 μM) over 72 h, followed by boron analysis by means of inductively coupled plasma (ICP) MS, revealed that the zwitterionic species **8** was taken up by the cells approximately twice as effectively as its charged *closo*-carborane analogue **7** (Fig. 8). We postulate that **8** can traverse the cell membrane more readily as a result of its neutral charge, leading to a more effective accumulation within the cell. Furthermore, there exist a series of organic cation and anion transporters in cells and these may play an important role in the differential uptake of **7** and **8** and their subsequent detoxification [37–39]. Incubating cells with a threefold higher concentration of **8** did not result in any increase in boron uptake (Fig. 8). Although the exact mechanism for the observed toxicity of these compounds is unknown, the more cytotoxic, cationic species **7** is the more likely of the two compounds to be taken up by the mitochondria and ultimately result in apoptosis; further investigation of the cellular organelle(s) targeted by these drugs will be reported in due course. The addition of **7** (10 μM) to T98G cells delivered approximately 1 order of magnitude more boron atoms to the cells than the boronic acid **1** at an identical dose (Fig. 8). Although cellular boron levels are much higher when a boron-rich carborane species is used, the intracellular concentration of **1** must be similar to that of **7** since the latter contains 10 times as many boron atoms per molecule. Moreover, the uptake of **8** is significantly greater than that of either **1** or **7**, in addition to **8** being the least cytotoxic agent in vitro. Lipophilicity appears to play only a minor role in cellular uptake of these agents as the extent of accumulation of boronic acid **1** was found to be similar to that of the *closo*-carborane species **7** (Fig. 8), with an uptake ratio of 1:1.1. A correlation of lipophilicity involving the boronic acid **1** and pinacol ester **2** with regard to cellular uptake cannot be made as **2** was found to readily hydrolyze during its crystallization to afford **1′** (vide supra) and so the boron uptake results pertaining to **2** may actually be the result of its partial or complete hydrolysis to **1** in aqueous solution.

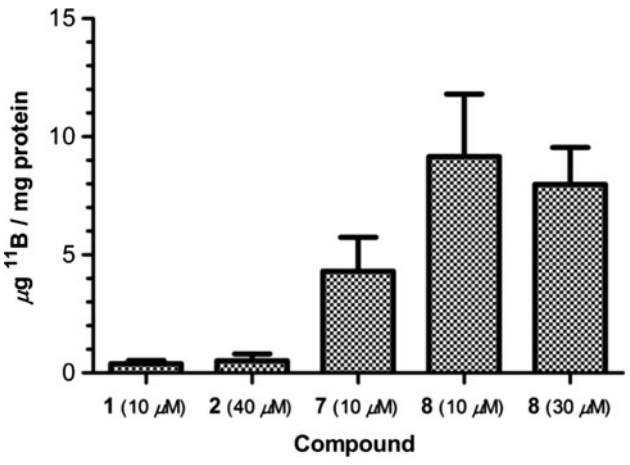

Fig. 8 Inductively coupled plasma mass spectrometry determination of boron uptake in human glioblastoma cells (T98G) treated with compounds **1**, **2**, **7**, and **8**

Conclusions

A series of novel boronated phosphonium salts have been synthesized and characterized. These compounds contain either free benzylboronic acids (**1**, **3**, and **5**), the corresponding boronate esters (**2**, **4**, and **6**), or a boron-rich *closo*-1,2-carborane cage (**7**). The facile preparation of the zwitterionic *nido*-7,8-carborane species **8** from **7** has also been described. All compounds were fully characterized using multinuclear (^{1}H, ^{11}B, ^{13}C, and ^{31}P) 1D- and 2D-NMR spectroscopy, ESI-MS, and elemental analysis, and single-crystal X-ray diffraction studies were also performed in the case of **1**, **3**, **7**, and **8**. In vitro cytotoxicity and uptake studies demonstrated that the boronated phosphonium salts were taken up by cultured T98G cells to a similar extent, regardless of the nature of the boron substituent(s), and all compounds were found to be significantly less toxic toward cultured MDCK II cells. However, the boron-rich carborane derivatives—the zwitterionic **8** in particular—possess the distinct advantage of delivering greater amounts of boron to the tumor cells on a per mole basis when compared with the related boronic acids/boronate esters. Furthermore, the accumulation of **8** was found to be approximately two-fold higher than that of the analogous species **7** and it exhibited a lower cytotoxicity than the corresponding *closo*-carborane species or the boronic acid derivatives. An investigation of whether the boronated phosphonium salts described in this work do indeed target mitochondria and affect their function like other DLCs is currently under way.

Materials and methods

nido-Decaborane(14) ($B_{10}H_{14}$) was purchased from Katchem (Czech Republic), and 2-(bromomethyl)phenylboronic acid, 3-(bromomethyl)phenylboronic acid, and 4-(bromomethyl)phenylboronic acid were purchased from Boron Molecular (Australia). All other reagents were

purchased from Aldrich. MeCN was freshly distilled from CaH_2 before use [40]. All other solvents were used without prior purification.

^{1}H, $^{13}C\{^{1}H\}$, and $^{31}P\{^{1}H\}$ NMR spectra were recorded at 27 °C using a Bruker Avance300 spectrometer (^{1}H at 300 MHz, ^{13}C at 75 MHz, ^{31}P at 121 MHz). $^{11}B\{^{1}H\}$ NMR spectra were recorded at 27 °C using a Bruker DRX400 spectrometer at 128 MHz. NMR signals (δ) are reported in parts per million. ^{1}H and $^{13}C\{^{1}H\}$ NMR spectra were referenced to the solvent residual peaks. $^{11}B\{^{1}H\}$ NMR spectra were referenced to external $BF_3{\cdot}OEt_2$ (0 ppm). $^{31}P\{^{1}H\}$ NMR spectra were referenced to external $P(OMe)_3$ (140.85 ppm). Low-resolution ESI-MS spectra were recorded using a Finnigan LCQ mass spectrometer. High-resolution ESI Fourier Transform ion cyclotron resonance MS data were recorded using a Bruker 7.0 T mass spectrometer. Elemental analyses were performed by the Campbell Microanalytical Laboratory, University of Otago, New Zealand.

General synthetic procedure for boronic acid derivatives

A solution containing 2-(bromomethyl)phenylboronic acid, 3-(bromomethyl)phenylboronic acid, or 4-(bromomethyl) phenylboronic acid (or their respective pinacol esters) and PPh_3 (1.1 mol equiv) in MeCN (20 mL) was stirred at 85 °C for 12 h [41]. The solvent was removed in vacuo and the residue was triturated with diethyl ether to yield a white precipitate that was collected by filtration and recrystallized from EtOH:Et_2O (1:1 v/v) to afford the desired product.

(4-Boronobenzyl)triphenylphosphonium bromide, ***1***

This compound was prepared using 4-(bromomethyl) phenylboronic acid (**9**; 0.29 g, 1.3 mmol) to give **1** (0.57 g, 1.2 mmol) as a colorless powder. Yield 0.57 g (89%). Melting point 210–212 °C. ^{1}H NMR [$CDCl_3$/dimethly-d_6 sulfoxide (d_6-DMSO)] δ 7.87 (t, 3H, Ph, $^{3}J_{H-H} = 7.41$ Hz), 7.68 (m, 9H, Ph), 7.56 (dd, 5H, Ph, $^{3}J_{H-H} = 7.92$ Hz, $^{3}J_{H-P} = 12.5$ Hz), 7.39 (br, 2H, BOH), 6.93 (dd, 2H, Ph, $^{3}J_{H-H} = 7.89$ Hz, $^{4}J_{H-P} = 2.0$ Hz), 4.89 (d, 2H, CH_2, $^{2}J_{H-P} = 14.9$ Hz). $^{13}C\{^{1}H\}$ NMR ($CDCl_3$/d_6-DMSO) δ 135.1 (d, Ph, $^{4}J_{C-P} = 2.3$ Hz), 134.6 (d, Ph, $^{3}J_{C-P} = 2.8$ Hz), 134.0 (d, Ph, $^{3}J_{C-P} = 9.7$ Hz), 130.0 (d, Ph, $^{2}J_{C-P} = 12.4$ Hz), 128.8 (d, Ph, $^{2}J_{C-P} = 8.5$ Hz), 117.6 (d, Ph, $^{1}J_{C-P} = 85.3$ Hz), 29.5 (d, CH_2, $^{1}J_{C-P} = 46.6$ Hz). $^{31}P\{^{1}H\}$ NMR ($CDCl_3$/d_6-DMSO) δ 28.4 (s). $^{11}B\{^{1}H\}$ NMR (d_6-DMSO) δ 27 (br, s). ESI-MS: *m/z* 411.33 ($[M + CH_3OH–H_2O–Br^-]^+$), 425.20 ($[M + 2CH_3OH–2H_2O–Br^-]^+$). Found: (%) C 62.69, H 4.90. Calc. for $C_{25}H_{23}BO_2PBr$: (%) C 62.93, H 4.86.

Triphenyl(4-(4,4,5,5-tetramethyl-1,3,2-dioxaborolan-2-yl)benzyl)phosphonium bromide, ***2***

This compound was prepared using 4-(bromomethyl) phenylboronic pinacol ester (**12**; 0.574 g, 1.93 mmol) to give **2** (1.08 g, 97%) as a colorless powder. Melting point 259–261 °C. ^{1}H NMR ($CDCl_3$) δ 7.75 (m, 9H, Ph), 7.64 (dd, 5H, Ph, $^{3}J_{H-H} = 7.17$ Hz, $^{4}J_{H-P} = 3.9$ Hz), 7.60 (d, 1H, Ph, $^{4}J_{H-P} = 3.6$ Hz), 7.55 (d, 2H, Ph, $^{3}J_{H-H} = 7.59$ Hz), 7.06 (dd, 2H, Ph, $^{3}J_{H-H} = 7.89$ Hz, $^{4}J_{H-P} = 2.1$ Hz), 5.41 (d, 2H, CH_2, $^{2}J_{H-P} = 14.7$ Hz), 1.32 (s, 12H, CH_3). $^{13}C\{^{1}H\}$ NMR ($CDCl_3$) δ 135.2 (m, Ph), 134.5 (d, Ph, $^{3}J_{C-P} = 9.7$ Hz), 130.9 (d, Ph, $^{4}J_{C-P} = 5.4$ Hz), 130.3 (d, Ph, $^{2}J_{C-P} = 12.5$ Hz), 117.9 (d, Ph, $^{1}J_{C-P} = 85.1$ Hz), 84.2 (s, COB), 31.4 (d, CH_2, $^{1}J_{C-P} = 46.7$ Hz), 25.0 (s, CH_3). $^{31}P\{^{1}H\}$ NMR ($CDCl_3$) δ 24.2 (s). $^{11}B\{^{1}H\}$ NMR ($CDCl_3$) δ 30 (br, s). ESI-MS: *m/z* 479.27 ($[M–Br^-]^+$), 1,039.07 ($[2M–Br^-]^+$), 1,071.07 ($[2M + CH_3OH–Br^-]^+$). Found: (%) C 64.87, H 6.08. Calc. for $C_{31}H_{33}BO_2PBr{\cdot}H_2O$: (%) C 64.50, H 6.11.

(3-Boronobenzyl)triphenylphosphonium bromide, ***3***

This compound was prepared using 3-(bromomethyl) phenylboronic acid (**10**; 0.50 g, 2.3 mmol) to give **3** as a colorless, crystalline solid. Yield 0.90 g (83%). Melting point 205–207 °C. ^{1}H NMR (d_6-DMSO) δ 7.92 (m, 5H, Ph/BOH), 7.74 (dt, 7H, Ph, $^{3}J_{H-H} = 7.80$ Hz, $^{4}J_{H-P} = 3.6$ Hz), 7.65 (dd, 6H, Ph, $^{3}J_{H-H} = 7.56$ Hz, $^{3}J_{H-P} = 12.3$ Hz), 7.47 (br, 1H, Ph), 7.18 (t, 1H, Ph, $^{3}J_{H-H} = 7.53$ Hz), 6.96 (d, 1H, Ph, $^{3}J_{H-H} = 7.35$ Hz), 5.14 (d, 2H, CH_2, $^{2}J_{H-P} = 15.6$ Hz). $^{13}C\{^{1}H\}$ NMR (d_6-DMSO) δ 137.0 (d, Ph, $^{3}J_{C-P} = 5.6$ Hz), 135.0 (s, Ph), 134.0 (d, Ph, $^{3}J_{C-P} = 9.8$ Hz), 132.3 (d, Ph, $^{3}J_{C-P} = 5.0$ Hz), 130.0 (d, Ph, $^{2}J_{C-P} = 12.3$ Hz), 127.7 (d, Ph, $^{4}J_{C-P} = 2.1$ Hz), 126.8 (d, Ph, $^{2}J_{C-P} = 8.5$ Hz), 117.8 (d, Ph, $^{1}J_{C-P} = 84.9$ Hz), 28.3 (d, CH_2, $^{1}J_{C-P} = 45.4$ Hz). $^{31}P\{^{1}H\}$ NMR (d_6-DMSO) δ 24.3 (s). $^{11}B\{^{1}H\}$ NMR (d_6-DMSO) δ 30 (br, s). ESI-MS: *m/z* 411.27 ($[M + CH_3OH–H_2O–Br^-]^+$), 425.20 ($[M + 2CH_3OH–2H_2O–Br^-]^+$). Found: (%) C 62.84, H 4.93. Calc. for $C_{25}H_{23}BO_2PBr$: (%) C 62.93, H 4.86.

Triphenyl(3-(4,4,5,5-tetramethyl-1,3,2-dioxaborolan-2-yl) benzyl)phosphonium bromide, ***4***

This compound was prepared using 3-(bromomethyl) phenylboronic pinacol ester (**13**; 0.652, 2.20 mmol) to give **4** as a colorless powder. Yield 1.21 g (97%). Melting point 265–267 °C. ^{1}H NMR ($CDCl_3$) δ 7.75 (m, 9H, Ph), 7.63 (m, 7H, Ph), 7.55 (d, 1H, Ph, $^{3}J_{H-H} = 7.68$ Hz), 7.20 (t, 1H, Ph, $^{3}J_{H-H} = 7.50$ Hz), 7.06 (br, 1H, Ph), 5.38 (d, 2H, CH_2, $^{2}J_{H-P} = 14.2$ Hz), 1.26 (s, 12H, CH_3). $^{13}C\{^{1}H\}$

NMR ($CDCl_3$) δ 137.3 (d, Ph, $^3J_{C-P} = 5.2$ Hz), 135.1 (d, Ph, $^4J_{C-P} = 2.6$ Hz), 134.8 (d, Ph, $^3J_{C-P} = 5.7$ Hz), 134.7 (d, Ph, $^4J_{C-P} = 3.7$ Hz), 134.4 (d, Ph, $^3J_{C-P} = 9.7$ Hz), 130.2 (d, Ph, $^2J_{C-P} = 12.5$ Hz), 128.6 (d, Ph, $^5J_{C-P} = 3.0$ Hz), 126.2 (d, Ph, $^2J_{C-P} = 8.5$ Hz), 117.7 (d, Ph, $^1J_{C-P} = 85.2$ Hz), 83.9 (s, COB), 31.1 (d, CH_2, $^1J_{C-P} = 46.8$ Hz), 24.8 (s, CH_3). $^{31}P\{^1H\}$ NMR ($CDCl_3$) δ 24.4 (s). $^{11}B\{^1H\}$ NMR ($CDCl_3$) δ 30 (br, s). ESI-MS: *m/z* 479.33 ($[M–Br^-]^+$), 1,038.73 ($[2M–Br^-]^+$), 1,070.93 ($[2M + CH_3OH–Br^-]^+$). Found: (%) C 65.88, H 6.04. Calc. for $C_{31}H_{33}BO_2PBr{\cdot}0.5H_2O$: (%) C 65.52, H 6.03.

(2-Boronobenzyl)triphenylphosphonium bromide, ***5***

This compound was prepared using 2-(bromomethyl) phenylboronic acid (**11**; 0.44 g, 2.0 mmol) to give **5** (0.92 g, 1.9 mmol) as a pale-yellow residue, which was recrystallized from EtOH to afford a colorless powder. Yield 0.92 g (94%). Melting point 224–226 °C. ^1H NMR (d_6-DMSO) δ 8.08 (s, 2H, BOH), 7.88 (t, 3H, Ph, $^3J_{H-H} = 7.37$ Hz), 7.70 (dt, 7H, $^3J_{H-H} = 7.74$ Hz, $^4J_{H-P} = 3.3$ Hz), 7.49 (dd, 6H, Ph, $^3J_{H-H} = 7.62$ Hz, $^3J_{H-P} = 12.4$ Hz), 7.31 (m, 2H, Ph), 7.04 (m, 1H, Ph), 5.38 (d, 2H, CH2, $^2J_{H-P} = 15.6$ Hz). $^{13}C\{^1H\}$ NMR (d_6-DMSO) δ 136.1 (d, Ph, $^4J_{C-P} = 2.4$ Hz), 135.0 (d, Ph, $^5J_{C-P} = 2.2$ Hz), 134.0 (d, Ph, $^3J_{C-P} = 9.6$ Hz), 133.2 (d, Ph, $^3J_{C-P} = 9.0$ Hz), 130.6 (d, Ph, $^3J_{C-P} = 5.0$ Hz), 130.3 (d, Ph, $^4J_{C-P} = 3.0$ Hz), 130.0 (d, Ph, $^2J_{C-P} = 12.2$ Hz), 127.5 (d, Ph, $^4J_{C-P} = 3.6$ Hz), 117.8 (d, Ph, $^1J_{C-P} = 84.9$ Hz), 28.4 (d, Ph, $^1J_{C-P} = 45.9$ Hz). $^{31}P\{^1H\}$ NMR (d_6-DMSO) δ 25.1 (s). $^{11}B\{^1H\}$ NMR (d_6-DMSO) δ 27 (br, s). ESI-MS: *m/z* 411.27 ($[M + CH_3OH–H_2O–Br^-]^+$), 425.20 ($[M + 2CH_3OH–2H_2O–Br^-]^+$). Found: (%) C 62.90, H 5.12. Calc. for $C_{25}H_{23}BO_2PBr$: (%) C 62.93, H 4.86.

Triphenyl(2-(4,4,5,5-tetramethyl-1,3,2-dioxaborolan-2-yl) benzyl)phosphonium bromide, ***6***

This compound was prepared using 2-(bromomethyl) phenylboronic pinacol ester (**14**; 0.44 g, 1.5 mmol) to afford **6** as a colorless solid. Yield 0.81 g (97%). Melting point 229–231 °C. ^1H NMR ($CDCl_3$) δ 7.78 (t, 4H, Ph, $^3J_{H-H} = 6.89$ Hz), 7.61 (dt, 8H, Ph, $^3J_{H-H} = 7.79$ Hz, $^4J_{H-P} = 3.4$ Hz), 7.49 (dd, 5H, Ph, $^3J_{H-H} = 7.89$ Hz, $^3J_{H-P} = 12.4$ Hz), 7.30 (br, 1H, P), 7.29 (s, 1H, Ph), 5.63 (d, 2H, CH_2, $^2J_{H-P} = 15.0$ Hz), 1.09 (s, 12H, CH_3). $^{13}C\{^1H\}$ NMR ($CDCl_3$) δ 137.2 (d, Ph, $^4J_{C-P} = 2.8$ Hz), 135.0 (d, Ph, $^4J_{C-P} = 2.6$ Hz), 134.2 (d, Ph, $^3J_{C-P} = 9.6$ Hz), 133.7 (d, Ph, $^3J_{C-P} = 9.1$ Hz), 132.1 (d, Ph, $^4J_{C-P} = 3.5$ Hz), 130.9 (d, Ph, $^3J_{C-P} = 4.9$ Hz), 130.0 (d, Ph, $^2J_{C-P} = 12.4$ Hz), 127.9 (d, Ph, $^4J_{C-P} = 3.8$ Hz), 117.6 (d, Ph, $^1J_{C-P} = 85.3$ Hz), 84.0 (s, COB), 30.3 (d, CH_2, $^1J_{C-P} = 46.1$ Hz), 24.7 (s, CH_3). $^{31}P\{^1H\}$ NMR ($CDCl_3$) δ 24.9 (s). $^{11}B\{^1H\}$ NMR ($CDCl_3$) δ 29.8 (br, s). ESI-MS: *m/z* 479.27 ($[M–Br^-]^+$), 1,039.00 ($[2M–Br^-]^+$), 1,070.67 ($[2M + CH_3OH–Br^-]^+$). Found: (%) C 64.83, H 5.77. Calc. for $C_{31}H_{33}BO_2PBr{\cdot}H_2O$: (%) C 64.50, H 6.11.

(Closo-1,2-carboran-1-ylmethyl)triphenylphosphonium bromide, ***7***

A stirred mixture of 1-bromomethyl-*closo*-1,2-carborane (**15**; 5.30 g, 22.3 mmol) and PPh_3 (6.50 g, 24.8 mmol) was heated to 100 °C in the absence of solvent for 4 days. The mixture was then cooled and triturated with Et_2O to yield **7** as a colorless solid. The unreacted starting materials were isolated from the Et_2O and recycled. Overall yield 1.77 g (15.9%). Melting point above 350 °C (decomposed). ^1H NMR ($CDCl_3$) δ 8.09 (dd, 6H, Ph, $^3J_{H-H} = 7.71$ Hz, $^3J_{H-P} = 12.9$ Hz), 7.83 (dt, 3H, Ph, $^3J_{H-H} = 7.50$ Hz, $^5J_{H-P} = 2.0$ Hz), 7.73 (dt, 6H, Ph, $^3J_{H-H} = 7.68$ Hz, $^4J_{H-P} = 3.6$ Hz), 6.14 (br, 1H, C–H cage), 5.60 (d, 2H, CH_2, $^2J_{H-P} = 14.3$ Hz), 3.4–0.8 (v. br, 10H, B–H cage). $^{13}C\{^1H\}$ NMR ($CDCl_3$) δ 135.7 (d, Ph, $^4J_{C-P} = 2.8$ Hz), 134.3 (d, Ph, $^3J_{C-P} = 10.4$ Hz), 130.7 (d, Ph, $^2J_{C-P} = 12.9$ Hz), 117.6 (d, Ph, $^1J_{C-P} = 86.5$ Hz), 66.7 (s, CH cage), 65.3 (s, C cage), 30.9 (d, CH_2, $^1J_{C-P} = 53.2$ Hz). $^{31}P\{^1H\}$ NMR ($CDCl_3$) δ 22.8 (s). $^{11}B\{^1H\}$ ($CDCl_3$) δ −2.7 (br, s), −9.3 (br, s), −12.0 (br, s). ESI-MS: *m/z* 419.40 ($[M–Br^-]^+$), 918.20 ($[2M–Br^-]^+$). Found: (%) C 50.57, H 5.83. Calc. for $C_{21}H_{28}B_{10}PBr$: (%) C 50.50, H 5.65.

(7,8-Dicarba-nido-undecaborane-7-ylmethyl) triphenylphosphonium zwitterion, ***8***

A solution of **7** (0.363 g, 0.727 mmol) and CsF (0.360 g, 2.37 mmol) in EtOH was stirred at reflux for 24 h. The solvent was removed in vacuo to afford a colorless solid. To this residue was added acetone (10 mL) and the insoluble borate products were filtered off. The acetone was removed in vacuo and the crude material was recrystallized in MeOH to afford **8** as a colorless solid (0.18 g, 61%). Melting point 297–299 °C. ^1H NMR (d_6-acetone) δ 7.95 (dd, 6H, Ph, $^3J_{H-H} = 7.38$ Hz, $^3J_{H-P} = 12.6$ Hz), 7.90 (dt, 3H, Ph, $^3J_{H-H} = 7.53$ Hz, $^5J_{H-P} = 2.0$ Hz), 7.77 (dt, 6H, Ph, $^3J_{H-H} = 7.77$ Hz, $^4J_{H-P} = 3.3$ Hz), 4.18 (dd, 1H, CH_2, $^2J_{H-H} = 16.44$ Hz, $^2J_{H-P} = 11.9$ Hz), 3.62 (dd, 1H, CH_2, $^2J_{H-H} = 16.50$ Hz, $^2J_{H-P} = 10.7$ Hz), 2.8 to −0.8 (v br, 9H, BH cage), 1.67 (br, 1H, CH cage), −3.60 (br, 1H, endo H). $^{13}C\{^1H\}$ NMR (d_6-acetone) δ 135.9 (d, Ph, $^4J_{C-P} = 2.8$ Hz), 135.4 (d, Ph, $^3J_{C-P} = 9.9$ Hz), 131.2 (d, Ph, $^2J_{C-P} = 12.3$ Hz), 121.3 (d, Ph, $^1J_{C-P} = 84.7$ Hz), 79.9 (s, CH cage), 79.19 (d, C cage, $^2J_{C-P} = 32.7$ Hz), 36.2 (d, CH_2, $^1J_{C-P} = 53.2$ Hz). $^{31}P\{^1H\}$ NMR (d_6-acetone) δ 23.4

(s). $^{11}B\{^{1}H\}$ NMR (d_6-acetone) δ –8.5 (br, s), –10.5 (br, s), –12.3 (br, s), –18.9 (br, s), –20.1 (br, s), –31.4 (br, s), –35.3 (br, s). ESI-MS: m/z 408.13 ($[M]^{-+}$). Found: (%) C 61.75, H 6.65. Calc. for $C_{21}H_{28}B_9P$: (%) C 61.71, H 6.91.

X-ray crystal structure determinations

A suitable single crystal was selected under a polarizing microscope (Leica M165Z) and was glued to a glass fiber with a dot of silicon paste that fixed the crystal firmly upon freezing at the temperature of data collection (−123 °C). The intensities were measured with a Bruker kappa APEXII CCD diffractometer equipped with graphite monochromated Mo Kα radiation ($\lambda = 0.71073$ Å) and operating at a low temperature of −173(2) °C maintained using an Oxford Cryosystems Cryostream 700 system. Upon obtaining an initial refinement of unit-cell parameters, the data collection strategy achieved a redundancy of at least 4 throughout the resolution range (from infinity to 0.80 Å) at 10-s exposure time per frame making use of the κ offsets on the four-circle goniometer geometry. The data integration and reduction with the multiscan absorption correction method was carried out using the APEX2 [42] software suite. The structure was solved by direct methods using SHELXS-97 [43] and was refined by the full-matrix least-squares refinement program SHELXL [43] to the final R value. All non-hydrogen atoms were refined anisotropically. The hydrogen atoms were located in the difference Fourier map, and some were fixed in their positions. Molecular graphics were generated using ORTEP-3v2. Key crystallographic data and refinement details are shown in Table 4.

Crystallographic data (without structure factors) for the structures reported in this paper have been deposited with the Cambridge Crystallographic Data Centre (CCDC) as supplementary publication nos. CCDC-768191 (compound **1′**), CCDC-768192 (compound **1**), CCDC-768193 (compound **3**), CCDC-68194 (compound **7**), and CCDC-768195 (compound **8**). Copies of the data can be obtained free of charge from the CCDC (12 Union Road, Cambridge CB2 1EZ, UK; Tel: +44-1223-336408; Fax: +44-1223-336003; e-mail: deposit@ccdc.cam.ac.uk).

In vitro cytotoxicity and cell uptake studies

Human glioblastoma multiforme (T98G) cells were maintained as monolayers in minimum essential medium supplemented with 10% fetal bovine serum, penicillin (100 units/mL), streptomycin (100 g/mL) and L-glutamine (2.5 mM), at 37 °C in a humidified 5% CO_2 atmosphere. MDCK II cells were maintained as monolayers in Dulbecco's modified Eagle's medium/Ham's F12 mixture supplemented with 10% fetal bovine serum, penicillin (100 units/mL), streptomycin (100 g/mL), and L-glutamine (2.5 mM), at 37 °C in a humidified 5% CO_2 atmosphere.

Cytotoxicity assays

Cytotoxicity was assessed using the 3-(4,5-dimethylthiazol-2-yl)-2,5-diphenyltetrazolium bromide (MTT) assay [44, 45]. Briefly, cells were harvested with trypsin (0.1% v/v), and cell pellets were isolated by centrifugation. Cells were then resuspended to a single cell suspension, cell numbers were counted using a hemocytometer (Weber), and then cells were seeded (density 1×10^4 cells per well) in growth medium (100 μL) using 96-well plates and were allowed to adhere overnight at 37 °C. Cells were incubated at 37 °C in a humidified atmosphere of 5% CO_2 in the presence of compounds **1**, **2**, **7**, and **8**, and the vehicle (control). Serial dilutions of boron compound were added to quadruplicate wells. After 72 h, MTT solution in phosphate-buffered saline (PBS; 20 μL, 0.25% w/v) was added and the incubation was continued. After a further 4 h, the culture medium and excess MTT solution were removed and the resulting MTT–formazan crystals dissolved by addition of 150 μL DMSO.

Cell viability was determined by measuring the absorbance at either 595 or 600 nm using an Ultramark multiwavelength plate reader (Bio-Rad, Australia) or a Victor$_3$V microplate reader (PerkinElmer), respectively. All readings were corrected for absorbance from wells containing the vehicle alone, and the level of MTT was expressed relative to the corresponding vehicle-treated controls as percent viability. Corresponding IC_{50} values for each of the compounds tested were then determined at the dose required to induce a 50% decrease in cell viability. All experiments were conducted at least in triplicate and all IC_{50} values are reported with standard errors where possible.

Cell uptake studies

Stock solutions of **1** and **2** (20 mM in DMSO), **7** (5 mM in EtOH), and **8** (5 mM in DMSO) were prepared. Warm (37 °C) culture medium was treated with the stock boron solutions to final concentrations of 10, 30, and 40 μM. The T98G cells were cultured as a monolayer in 75-cm^2 flasks to 70–80% confluence and then incubated with the boron-containing culture medium at the respective concentrations for 72 h at 37 °C in a humidified 5% CO_2 atmosphere. The medium was removed and the cells were washed once with PBS (2 mL). PBS (4 mL) was added to the culture flask and then cells were harvested with a rubber policeman, rinsing with further PBS (2 mL). Harvested cells were pipetted until a single cell suspension was achieved, which was then divided into aliquots (100 μL) for protein analysis. The remaining cells were sedimented by

Table 4 Crystal data for compounds **1**, **3**, **7**, and **8**

	1	**3**	**7**	**8**
Crystal data				
Chemical formula	$C_{25}H_{23}BBrO_2P$	$C_{25}H_{23}BBrO_2P$	$C_{21}H_{28}B_{10}BrP$	$C_{21}H_{28}B_9P$
M_r	477.12	477.12	499.41	408.69
Cell setting, space group	Triclinic, *P*-1	Monoclinic, *Pn*	Monoclinic, *P*2(1)/*n*	Orthorhombic, *P*2(1)2(1)2(1)
Temperature (°C)	−123(2)	−123(2)	−123(2)	−123(2)
a, *b*, *c* (Å)	9.3253(3), 10.0392(3), 12.7552(4)	9.8364(7), 9.4813(6), 12.0475(7)	11.2209(3), 11.7646(4), 19.7629(6)	8.9605(12), 14.892(2), 17.136(2)
α, β, γ (°)	73.8260(10), 74.7010(10), 88.8710(10)	90, 94.761(2), 90	90, 103.8710(10), 90	90, 90, 90
V (Å^3)	1,104.35(6)	1,119.70 (12)	2,532.81(13)	2,286.7(5)
Z	2	2	4	4
D_x (Mg m^{-3})	1.435	1.415	1.31	1.187
Radiation type	Mo Kα	Mo Kα	Mo Kα	Mo Kα
μ (mm^{-1})	1.95	1.93	1.7	0.13
Crystal form, color	Cubic, colorless	Plates, colorless	Blocks, colorless	Blocks, colorless
Crystal size (mm^3)	0.14 × 0.10 × 0.07	0.18 × 0.08 × 0.04	0.23 × 0.19 × 0.11	0.20 × 0.16 × 0.13
Data collection				
Diffractometer	Bruker kappa APEXII CCD area detector			
Data collection method	φ scans and ω scans with κ offsets			
Absorption correction	Multiscan			
T_{min}	0.777	0.726	0.694	0.975
T_{max}	0.882	0.936	0.83	0.983
No. of measured, independent and observed reflections	15,727, 3,879, 3,606	7,737, 3,740, 3,179	17,896, 4,439, 4,003	15,417, 3,994, 3,269
Criterion for observed reflections	$I > 2\sigma(I)$	$I > 2\sigma(I)$	$I > 2\sigma(I)$	$I > 2\sigma(I)$
R_{int}	0.042	0.071	0.055	0.053
q_{max} (°)	25	25	25	25
Refinement				
Refinement on	F^2	F^2	F^2	F^2
$R[F^2 > 2\sigma(F^2)]$, $wR(F^2)$, S	0.026, 0.089, 0.68	0.047, 0.129, 0.74	0.028, 0.097, 0.81	0.045, 0.130, 0.87
No. of reflections	3,879	3,740	4,439	3,994
No. of parameters	367	347	410	383
H-atom treatment	Mixture of independent and constrained refinement			
Weighting scheme	Calculated $w = 1/[\sigma^2(F_o^2) + (0.1P)^2 + 0.9602P]$, where $P = (F_o^2 + 2F_c^2)/3$			
$(\Delta/\sigma)_{max}$	0.001	<0.0001	0.001	<0.0001
$\Delta\rho_{max}$, $\Delta\rho_{min}$ (e^- Å^{-3})	0.79, –0.71	0.31, –0.32	0.36, –0.43	0.30, –0.31

centrifugation at 2,000 rpm for 3 min, then the supernatant was removed and the cell pellet was analyzed for boron content.

Microwave digestion and measurement of boron concentration by ICP-MS

As certified boron reference materials are not available, method control was performed by the determination of boron using an accurate weight of **1**, **2**, **7**, and **8**. For closed-system digestions, the determined recoveries were 103 ± 14% ($n = 3$), 93 ± 5% ($n = 3$), 94 ± 6% ($n = 3$), and 86 ± 7% ($n = 3$) for **1**, **2**, **7**, and **8**, respectively. The minor losses of boron can be attributed to volatilization and/or surface adsorption.

The cell pellets were transferred to precleaned TFM vessels with MQ water (2 × 0.25 mL) then dried for 1 h at 110 °C and cooled to room temperature. The cell pellets were suspended in HNO_3 (70%, 7.5 mL) and H_3PO_4 (85%, 2.5 mL) as described previously [46] and subjected to three high-pressure microwave digestion cycles using a Milestone Ethos Plus microwave laboratory station. The microwave digestion program involved heating to 200 °C over 10 min, holding for 10 min then heating to 240 °C

over 5 min, and sustaining this temperature for a further 20 min. Between program cycles, the closed sample vessels were cooled to 150–100 °C. At the end of the digestion process, the closed vessels were cooled to room temperature to minimize volatile analyte losses, and the resulting homogeneous solutions were diluted with MQ water to a final volume of 30 mL. ICP-MS analyses were performed using a PerkinElmer Elan DRCII ICP-MS system. Beryllium (20 ng/mL) was used as an internal standard by in-line injection and the ^{10}B and ^{11}B lines were analyzed. Standard solutions of boric acid were used to prepare a calibration plot. The introduction of D-mannitol (0.25% w/v) and aqueous ammonia (0.1 M) to all final samples/diluents and flush solutions is known to minimize boron carryover and memory effects [47]. However, it is also known to reduce instrument sensitivity, so no additives were used in ICP-MS analyses of these samples. Instead, all dilutions of samples/standards and flushes between ICP-MS runs were made with MQ water only. To account for any variations in total cell number, the measured boron content was normalized to cell protein measured in the corresponding cell preparations and expressed in units of micrograms of ^{11}B per milligram of protein, analyzed as described next.

Protein analyses

The bicinchoninic acid (BCA) protein assay was used to determine protein concentration, as described previously [48]. This assay relies on the reduction of alkaline Cu(II) by proteins. A bovine serum albumin (BSA) protein standard curve was prepared each time the assay was performed.

Lysis of cells was achieved using three snap freeze–thaw cycles and cell debris was sedimented by centrifugation at 13,300 rcf for 5 min. The supernatant solution was then analyzed for protein content by taking repeated 10- or 15-μL samples ($n = 3$) of the blank, 1 mg/mL BSA protein standard (200, 400, 800, and 1,000 μg/mL, made up to volume with MQ water) or boron-treated protein samples and depositing these into a 96-well plate format. Next, a freshly prepared solution of commercially sourced BCA and $CuSO_4 \cdot 5H_2O$ (50:1, 190 or 285 μL) was added to each well and the mixture was incubated at 37 °C for 60 min. Absorbance was then measured at 595 nm using an Ultramark multiwavelength plate reader (Bio-Rad, Australia) and was protein determined by comparison with the BSA standard curve.

Acknowledgments We gratefully acknowledge the assistance provided by Ian Luck (The University of Sydney) with the NMR studies, Keith Fisher (The University of Sydney) for collection of the ESI-MS data, and Dorothy Yu (ICP Analytical Centre, The University of New South Wales) for boron analysis. We are grateful to the Australian Research Council (ARC), Cure Cancer Foundation of Australia, and National Breast Cancer Foundation for financial support.

References

1. Barth RF, Coderre JA, Vicente MGH, Blue TE (2005) Clin Cancer Res 11:3987–4002
2. Crossley EL, Ziolkowski EJ, Coderre JA, Rendina LM (2007) Mini Rev Med Chem 7:303–313
3. Soloway AH, Tjarks W, Barnum BA, Rong F-G, Barth RF, Codogni IM, Wilson JG (1998) Chem Rev 98:1515–1562
4. Modica-Napolitano JS, Aprille JR (2001) Adv Drug Deliv Rev 49:63–70
5. Rowe TC, Weissig V, Lawrence JW (2001) Adv Drug Deliv Rev 49:175–187
6. Modica-Napolitano JS, Nalbandian R, Kidd ME, Nalbandian A, Nguyen CC (2003) Cancer Lett 198:59–68
7. Galeano E, Nieto E, Garcia-Perez Ana I, Delgado MD, Pinilla M, Sancho P (2005) Leuk Res 29:1201–1211
8. Johnson LV, Walsh ML, Chen LB (1980) Proc Natl Acad Sci USA 77:990–994
9. Modica-Napolitano JS, Aprille JR (1987) Cancer Res 47: 4361–4365
10. Modica-Napolitano JS, Koya K, Weisberg E, Brunelli BT, Li Y, Chen LB (1996) Cancer Res 56:544–550
11. Weiss MJ, Wong JR, Ha CS, Bleday R, Salem RR, Steele GD, Chen LB (1987) Proc Natl Acad Sci USA 84:5444–5448
12. Anderson WM, Delinck DL, Benninger L, Wood JM, Smiley ST, Chen LB (1993) Biochem Pharmacol 45:691–696
13. Sun X, Wong JR, Song K, Hu J, Garlid KD, Chen LB (1994) Cancer Res 54:1465–1471
14. Patel J, Rideout D, McCarthy MR, Calogeropoulou T, Wadwa KS, Oseroff AR (1994) Anticancer Res 14:21–28
15. Adams DM, Ji W, Barth RF, Tjarks W (2000) Anticancer Res 20:3395–3402
16. Calabrese G, Gomes ACNM, Barbu E, Nevell TG, Tsibouklis J (2008) J Mater Chem 18:4864–4871
17. Steichen JD, Weiss MJ, Elmaleh DR, Martuza RL (1991) J Neurosurg 74:116–122
18. Min J-J, Biswal S, Deroose C, Gambhir SS (2004) J Nucl Med 45:636–643
19. Davis S, Weiss MJ, Wong JR, Lampidis TJ, Chen LB (1985) J Biol Chem 260:13844–13850
20. Yokoyama K, Miyatake S-I, Kajimoto Y, Kawabata S, Doi A, Yoshida T, Asano T, Kirihata M, Ono K, Kuroiwa T (2006) J Neuro Oncol 78:227–232
21. Ioppolo JA, Clegg JK, Rendina LM (2007) Dalton Trans 1982–1985
22. Rideout DC, Calogeropoulou T, Jaworski JS, Dagnino R Jr, McCarthy MR (1989) Anticancer Drug Des 4:265–280
23. Hernandez P, Merlino A, Gerpe A, Porcal W, Piro OE, Gonzalez M, Cerecetto H (2006) ARKIVOC xi:128–136
24. Patel RM, Argade NP (2007) J Org Chem 72:4900–4904
25. Heying TL, Ager JW, Clark SL, Alexander RP, Papetti S, Reid JA, Trotz SI (1963) Inorg Chem 2:1097–1105
26. Grafstein D, Bobinski J, Dvorak J, Smith HF, Schwartz NN, Cohen MS, Fein MM (1963) Inorg Chem 2:1120–1125
27. Kalinin VN, Rys EG, Tyutyunov AA, Starikova ZA, Korlyukov AA, Ol'shevskaya VA, Sung DD, Ponomaryov AB, Petrovskii PV, Hey-Hawkins E (2005) Dalton Trans 903–908
28. Yoo J, Hwang J-W, Do Y (2001) Inorg Chem 40:568–570

29. Grim SO, McFarlane W, Davidoff EF, Marks TJ (1966) J Phys Chem 70:581–584
30. Malmquist J, Sjoeberg S (1992) Inorg Chem 31:2534–2537
31. Teixidor F, Angles P, Vinas C (1999) Inorg Chem 38:3605–3608
32. Valliant JF, Guenther KJ, King AS, Morel P, Schaffer P, Sogbein OO, Stephenson KA (2002) Coord Chem Rev 232:173–230
33. Ponnuswamy MN, Czerwinski EW (1986) Acta Crystallogr Sect C Crystallogr Struct Commun C 42:1019–1022
34. Batsanov AS, Davidson MG, Howard JAK, Lamb S, Lustig C (1996) Chem Commun 1791–1792
35. Holynska M, Lis T (2004) Acta Crystallogr Sect C Crystallogr Struct Commun C 60:m648–m650
36. Bergeron KL, Murphy EL, Majofodun O, Munoz LD, Williams JC Jr, Almeida KH (2009) Mutat Res Genet Toxicol Environ Mutagen 673:141–148
37. Girardin F (2006) Dialogues Clin Neurosci 8:311–321
38. Kerb R (2006) Cancer Lett 234:4–33
39. Sekine T, Cha SH, Endou H (2000) Eur J Physiol 440:337–350
40. Armarego WLF, Chai C (2003) Purification of laboratory chemicals, 5th edn. Butterworth–Heinemann, Oxford
41. Matteson DS, Man HW (1994) J Org Chem 59:5734–5741
42. Bruker (2007) Bruker Analytical X-ray Instruments, Madison
43. Sheldrick GM (2008) Acta Crystallogr Sect A Found Crystallogr A 64:112–122
44. Hall MD, Amjadi S, Zhang M, Beale PJ, Hambley TW (2004) J Inorg Biochem 98:1614–1624
45. Mosmann T (1983) J Immunol Methods 65:55–63
46. Probst TU, Berryman NG, Lemmen P, Weissfloch L, Auberger T, Gabel D, Carlsson J, Larsson B (1997) J Anal At Spectrom 12:1115–1122
47. Sun D-H, Ma R-L, McLeod CW, Wang X-R, Cox AG (2000) J Anal At Spectrom 15:257–261
48. Smith PK, Krohn RI, Hermanson GT, Mallia AK, Gartner FH, Provenzano MD, Fujimoto EK, Goeke NM, Olson BJ, Klenk DC (1985) Anal Biochem 150:76–85